

Crystal structure of the phosphatidylinositol-specific phospholipase C from *Bacillus cereus* in complex with *myo*-inositol

Dirk W.Heinz¹, Margret Ryan²,
Timothy L.Bullock^{2,3} and O.Hayes Griffith²

Institut für Organische Chemie und Biochemie, Universität Freiburg, D-79104 Freiburg, Germany and ²Institute of Molecular Biology, University of Oregon, Eugene, OR 97403, USA

³Present address: Structural Studies, MRC–LMB, Hills Road, Cambridge CB2 2QH, UK

¹Corresponding author

Phosphatidylinositol (PI), once regarded as an obscure component of membranes, is now recognized as an important reservoir of second messenger precursors and as an anchor for membrane enzymes. PI-specific phospholipase C (PI-PLC) is the enzyme that cleaves PI, invoking numerous cellular responses. The crystal structure of PI-PLC from *Bacillus cereus* (EC 3.1.4.10) has been solved at 2.6 Å resolution and refined to a crystallographic *R* factor of 18.7%. The structure consists of an imperfect ($\beta\alpha$)₈-barrel similar to that first observed for triose phosphate isomerase and does not resemble any other known phospholipase structure. The active site of the enzyme has been identified by determining the structure of PI-PLC in complex with its inhibitor, *myo*-inositol, at 2.6 Å resolution (*R* factor = 19.5%). This substrate-like inhibitor interacts with a number of residues highly conserved among prokaryotic PI-PLCs. Residues His32 and His82, which are also conserved between prokaryotic and eukaryotic PI-PLCs, most likely act as general base and acid respectively in a catalytic mechanism analogous to that observed for ribonucleases.

Keywords: catalytic mechanism/inhibitor complex/phosphatidylinositol/phospholipase C/three-dimensional structure

Introduction

The independent discoveries that phosphatidylinositols (PIs) are key players in signal transduction and that these lipids are also the anchor for numerous membrane-associated proteins have created vigorous activity in these fields (Berridge and Irvine, 1989; Rhee *et al.*, 1989; Turner, 1990). PI-specific phospholipase C (PI-PLC) is the class of ubiquitous enzymes that cleaves PI into the water-soluble *myo*-inositol 1:2-cyclic phosphate [I(1:2 cyc)P] or *myo*-inositol 1-phosphate [I(1)P] and the lipid-soluble diacylglycerol (DAG) (Figure 1). Thus PI-PLC is responsible for many of the biological functions of PI (Berridge and Irvine, 1989; Rhee *et al.*, 1989; Turner, 1990; Bruzik and Tsai, 1994). The smaller PI-PLCs are excreted by a variety of bacteria, including *Bacillus cereus* and the closely related insect pathogen *Bacillus thuringiensis* and by the animal and human pathogens

Staphylococcus aureus and *Listeria monocytogenes*, where PI-PLCs are potential virulence factors (Kuppe *et al.*, 1989; Leimeister-Wächter *et al.*, 1991; Mengaud *et al.*, 1991; Daugherty and Low, 1993). The parasite *Trypanosoma brucei* produces a glycosylphosphatidylinositol-specific phospholipase C (GPI-PLC), a subclass of PI-PLC which cleaves the GPI anchor of its variant surface glycoprotein coat (Hereld *et al.*, 1988; Carrington *et al.*, 1991), presumably facilitating the ability of the protozoan to defeat the host's immune system.

The larger members exist as several isoenzymes in eukaryotes, where they have a central role in PI-dependent transmembrane signal transduction by hormones and growth factors (Berridge and Irvine, 1989; Rhee *et al.*, 1989), cleaving the more highly phosphorylated derivatives of PI to form two second messengers, *myo*-inositol 1,4,5-trisphosphate (IP₃) and DAG.

Many of the prokaryotic and eukaryotic PI-PLCs have now been cloned and sequenced, but structural information is still lacking.

PI-PLC from *B.cereus* (EC 3.1.4.10) contains 298 amino acid residues (Kuppe *et al.*, 1989) and is the most widely used PI-PLC as a test for the presence of GPI-anchored proteins, since this PI-PLC has both GPI- and PI-cleaving activities (Turner, 1990; Ikezawa, 1991; Bruzik and Tsai, 1994). Here we report the structure determination of *B.cereus* PI-PLC in its free form and in complex with the inhibitor *myo*-inositol at 2.6 Å resolution and describe the first three-dimensional structure for a member of this family of enzymes.

Results and discussion

Quality of the model

The structure of *B.cereus* PI-PLC was solved by using multiple isomorphous replacement and crystallographic refinement (Table I and Figure 2). The final model, containing 2991 non-hydrogen protein atoms and 52 solvent molecules, has a crystallographic *R* factor of 18.7% ($R_{\text{free}} = 26.4\%$; Brünger, 1992) for data with $I/\sigma_I \geq 1$ between 8 and 2.6 Å resolution. The root mean square (r.m.s.) deviations are 0.01 Å from ideal bond lengths and 1.6° from ideal bond angles. The current model includes all residues except the C-terminal residues Lys297 and Glu298, which are flexible. The Ramachandran plot (Morris *et al.*, 1992) for the final model shows 83.3% of the residues in the most favored regions and none of the non-glycine residues in disallowed regions. All residues are in acceptable environments as determined from the three-dimensional–one-dimensional profile plots (Lüthy *et al.*, 1992) and energy graphs (Sippl, 1993). The structure of the complex between PI-PLC and *myo*-inositol was solved by difference Fourier calculations (Figure 3) and refined at 2.6 Å resolution. The current *R* factor for the

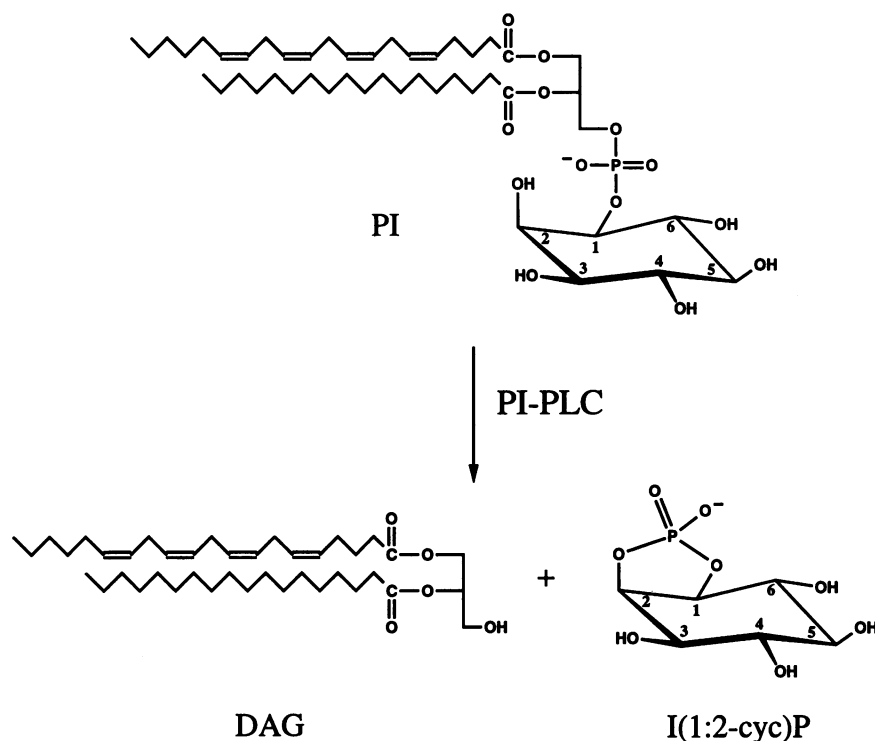


Fig. 1. The reaction catalyzed by *B.cereus* PI-PLC forming diacylglycerol (DAG) and *myo*-inositol 1:2-cyclic phosphate [I(1:2cyc)P]. In a second, much slower reaction, this enzyme converts I(1:2cyc)P to *myo*-inositol-1-phosphate (not shown).

Table I. Crystallographic statistics for native, complex and derivative data sets

Data set	Native	K162C– HgCl ₂ ^a	T185C– HgCl ₂	D224C– HgCl ₂	D139C– HgCl ₂	DMD ^b	PtCl ₂	TERPY ^c	PI-PLC– <i>myo</i> -inositol complex
Max. resolution (Å)	2.6	2.6	2.6	2.6	2.6	2.6	3.0	3.0	2.6
Unique reflections	9528	9818	9979	9069	10 213	10 112	6477	6537	8639
Completeness ^d	0.86 (0.62)	0.89 (0.74)	0.90 (0.73)	0.82 (0.56)	0.92 (0.73)	0.91 (0.71)	0.89 (0.80)	0.90 (0.80)	0.79 (0.58)
R_{merge}^e	0.064	0.055	0.072	0.074	0.078	0.065	0.058	0.060	0.045
R_{iso}^f		0.17	0.119	0.122	0.132	0.14	0.111	0.128	
Number of sites		1	4	4	4	3	4	3	
Phasing power ^g									
Centric		0.9	1.2	1.0	0.9	1.0	0.5	0.5	
Acentric		1.3	1.4	1.3	1.2	1.3	0.7	0.7	

^aK162C–HgCl₂ incitates a data set for the mutant K162C soaked with HgCl₂.

^bDMD, diacetoxy mercuridipropylene dioxide.

^cTERPY, chloro(2,2':6,2''-terpyridinium)platinum(II) chloride.

^dCompleteness is the ratio of the observed to the theoretically possible reflections. Values in parentheses are for the highest resolution shells.

^e $R_{\text{merge}} = \sum I_i - \langle I \rangle / \sum I_i$, where I_i is the intensity of an individual reflection and $\langle I \rangle$ is the mean intensity of that reflection.

^f $R_{\text{iso}} = \sum_{\text{hkl}} |F_{\text{nat}} - F_{\text{der}}| / \sum_{\text{hkl}} F_{\text{nat}}$, where F_{nat} and F_{der} are the structure amplitudes for native and derivative data sets respectively.

^gPhasing power = $\langle F_{\text{H}} \rangle / \langle E \rangle$, where $\langle F_{\text{H}} \rangle$ is the r.m.s. of the heavy atom scattering factor and $\langle E \rangle$ is the r.m.s. lack of closure; the summation is computed for reflections used in the heavy atom refinement cycle.

complex is 19.5%, with r.m.s. deviations of 0.015 Å from ideal bond lengths and 1.8° from ideal bond angles. The atomic coordinates of both structures have been deposited with the Brookhaven Protein Data Bank (Bernstein *et al.*, 1977).

Overall structure of PI-PLC

Bacillus cereus PI-PLC consists of a single globular domain with approximate dimensions 40×40×50 Å³. It folds as an imperfect (β α)₈-barrel with strong similarity to the ever increasing group of triose phosphate isomerase (TIM)-barrel-containing proteins (Farber, 1993), although

with a number of unique features (Figure 4). Only six instead of eight (β α) units are found in the barrel, lacking helices between strands IV and V and V and VI. The parallel eight-stranded β-barrel comprises residues 29–34 (strand I), 64–72 (II), 108–114 (III), 155–163 (IV), 173–176 (V), 193–201 (VI), 226–236 (VII) and 269–274 (VIII). The helices comprise residues 4–8 (helix A), 42–48 (B), 55–61 (C), 91–107 (D), 127–139 (E), 204–222 (F), 243–264 (G) and 284–294 (H). The β-barrel is not strictly closed, due to the absence of main chain hydrogen bonding interactions between β-strands V and VI. The hydrogen bonding potential of β-strand VI is partially satisfied by

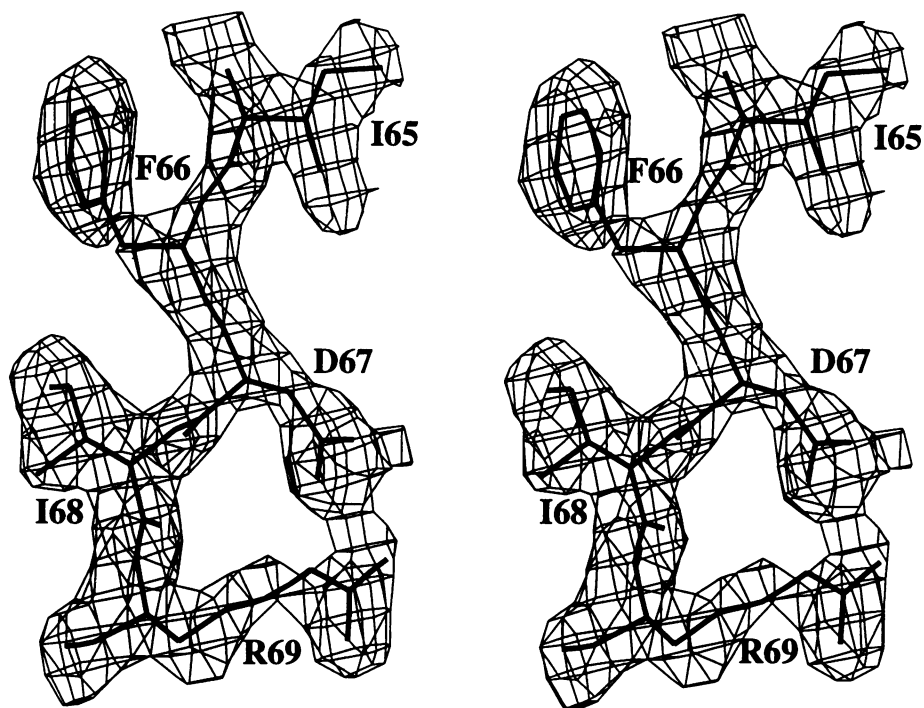


Fig. 2. Stereo picture of the final ($2F_o - F_c$) electron density map for residues 65–69 belonging to β -strand II of PI-PLC. Electron density is contoured at 1.3σ . Amino acid residues are labeled using the single letter code.

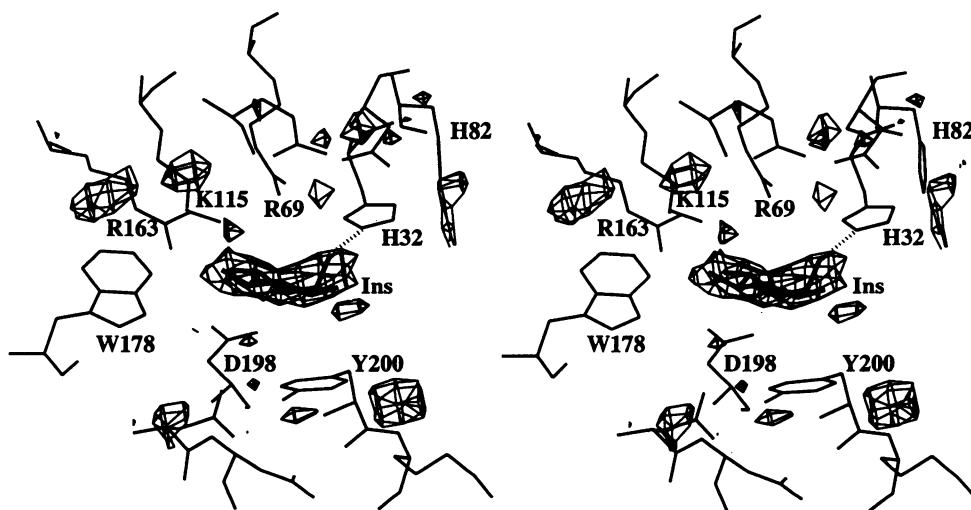


Fig. 3. Stereo picture showing the *myo*-inositol molecule (thick bonds, side view, labeled as Ins) bound to the active site of PI-PLC (thin bonds). Superimposed is the positive difference electron density between complexed and free PI-PLC. Residues in close contact with the inhibitor are labeled using the single letter code. The contour level is 2.5σ .

interactions with β -strand Vb (residues 182–188), which is, however, antiparallel to the central barrel. Most of the β -strands in PI-PLC are significantly longer than found in a typical TIM-barrel (Lesk *et al.*, 1989), reaching 11 residues for strand VII. The presence of an antiparallel β -strand and the absence of two α -helices has also been observed in the 'unusual' TIM-barrels found in both cellobiohydrolase II from *Trichoderma reesei* (Rouvinen *et al.*, 1990) and thermophilic endocellulase E2 from *Thermomonospora fusca* (Spezio *et al.*, 1993).

The PI-PLC is the first phospholipase with TIM-barrel topology. Therefore its structure does not show any similarity to the other phospholipase structures elucidated so far, i.e. phosphatidylcholine hydrolyzing phospholipase

C from *B. cereus* (Hough *et al.*, 1989) and phospholipases A2 (Retseder *et al.*, 1985; White *et al.*, 1990), which are both smaller and predominantly α -helical.

The active site and binding of *myo*-inositol

The active site is located in a wide and solvent-accessible cleft at the C-terminal end of the β -barrel (Figures 5 and 6), as observed for all TIM-barrel enzymes. The center of the cleft is lined by several polar and charged amino acids, intuitively suggesting a potential role in substrate binding and catalysis. The rim of the active site is formed by several loops, as well as the short helix B. This helix, as well as the loop comprising residues 237–243, shows an unusual clustering of hydrophobic amino acids that are

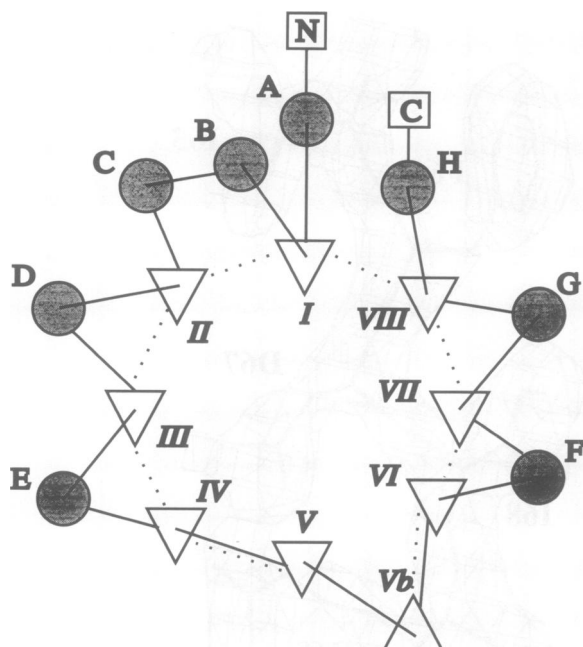


Fig. 4. Topology sketch of *B.cereus* PI-PLC. α -Helices (A–I) are symbolized by gray spheres, β -strands (I–VIII) by white triangles. N- and C-termini are marked by N and C respectively. In the orientation shown the direction of the strands belonging to the central parallel β -barrel points out of the plane of the paper. Main chain hydrogen bonding between β -strands is shown by dotted lines.

fully exposed to solvent. Two of the seven tryptophans (Trp47 and Trp242) are among these exposed hydrophobic amino acids. This structural information correlates well with the spectroscopic data of Volwerk *et al.* (1994), who observed that there are tryptophans in *B.cereus* PI-PLC which are exposed to the solvent and are sensitive to the binding to vesicles and micelles of phospholipids. These residues may contribute to the interfacial activation observed for *B.cereus* PI-PLC (Hendrickson *et al.*, 1992; Lewis *et al.*, 1993) and may also be involved in contacting the lipophilic part of PI. Both helix B and loop 237–243 are weakly defined in the electron density map, which could indicate their potential role as a flexible lid during attack on the phospholipid substrate by the enzyme.

In contrast to the phospholipases A₂, PI-PLC does not show stereospecificity towards the DAG moiety, suggesting that the hydrophobic part of PI is not specifically recognized by PI-PLC (Bruzik *et al.*, 1992). Inspection of the outer parts of the active site cleft of PI-PLC corroborates this observation. In this area the active site cleft is wide open and lined with rather small amino acids and therefore probably cannot discriminate between different stereoisomers of the glycerol moiety.

Myo-inositol is a weak competitive inhibitor of PI-PLC with an IC₅₀ of 8 mM (Shashidhar *et al.*, 1990). It binds to the deepest part of the active site cleft (Figure 5) and makes a number of well-defined hydrogen bonding interactions exclusively with charged side chains that are themselves held in place by a network of hydrogen bonding and electrostatic interactions with the protein (Figure 6). The binding of inositol to the active site did not induce any notable conformational changes in the enzyme. The hydroxyl groups at positions 1 and 6 of inositol (OH1 and OH6) are fully exposed to solvent and

do not form any hydrogen bonding interactions with the enzyme. This is not surprising, because both groups are replaced by more bulky groups in the PI-PLC substrates PI (a DAG phosphate moiety at OH1, see Figure 1) and GPI (a DAG phosphate at OH1 and a glycosaminoglycan moiety at OH6). The remaining hydroxyl groups form several specific hydrogen bonding interactions with the enzyme, as shown in Figure 7: OH2, which is the only axial hydroxyl group in inositol, to atoms N^{ε2} of His32 and N^{η2} of Arg69, OH3 to atom O^{δ1} of Asp198, OH4 to atoms N^{η1}, N^{η2} of Arg163 and O^{δ2} of Asp198 and OH5 to atoms N^ζ of Lys115 and N^{η2} of Arg163. Furthermore, there is a stacking interaction of the large apolar patch of the inositol ring with the phenol ring of Tyr200 and numerous other van der Waals interactions between the enzyme and inositol, leading to a partial enclosure of the inositol molecule within the binding site. All these features are characteristic of the active sites of monosaccharide binding proteins (Quiocho, 1989), which also show a high stereoselectivity for their substrates.

Catalytic mechanism of PI-PLC

Based on the presence of the stable catalytic intermediate I(1:2-cyc)P, a mechanism of general base and acid catalysis with two active site histidines, similar to the ribonuclease mechanism (Richards and Wyckhoff, 1971; Thompson and Raines, 1994), has been proposed for PI-PLC (Lin *et al.*, 1990; Volwerk *et al.*, 1990; Lewis *et al.*, 1993). From the structure of the complex between PI-PLC and inositol we identified the two potential catalytic histidines. His32 forms with its N^{ε2} atom a hydrogen bond with the OH2 group of inositol and is, therefore, the most likely candidate to act as a general base. The carboxyl group of Asp274 forms a hydrogen bond with the N^{δ1} atom of His32 and probably stabilizes the imidazole of His32 in the correct tautomeric state for base catalysis (Figure 7). Taken together, Asp274, His32 and the OH2 group of inositol form a 'catalytic triad' analogous to the well-known catalytic triads found in serine proteases and other hydrolases, however, in this case with the nucleophilic hydroxyl group provided by the substrate itself, instead of coming from the enzyme.

The only histidine located in the active site and in a suitable position to protonate the leaving group is His82, which is located ~4.7 Å away from the OH1 group of inositol.

We verified the essential role of both histidines in catalysis by site-directed mutagenesis. Replacement of either His32 or His82 with leucine led to inactive mutants. Both histidines are strongly conserved, not only among prokaryotic, but also eukaryotic PI-PLCs (including the GPI-PLC from *T.brucei*), despite weak overall homology (Suh *et al.*, 1988; Carrington *et al.*, 1991; Mengaud *et al.*, 1991; Daugherty and Low, 1993). The imidazole rings of both histidines are ~6 Å apart, a distance strikingly similar to that of the active histidine pair in ribonuclease A. In fact the superposition of both imidazole rings of His32 and His82 in PI-PLC with the equivalent histidine pair (His12 and His119) in ribonuclease A (Aguilar *et al.*, 1991) produces a very close overlap, although the main chain atom positions and the rest of the enzymes are very different (not shown). This is another example of convergent evolution, where two structurally unrelated

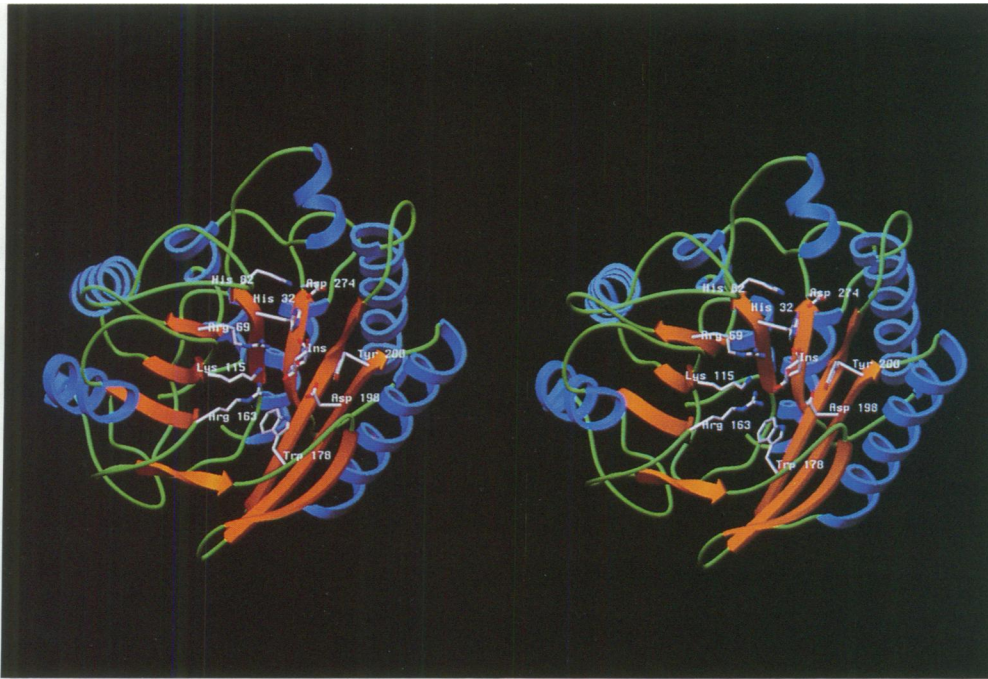


Fig. 5. Stereo ribbon diagram of *B.cereus* PI-PLC structure showing the active site pocket. α -Helices are depicted in blue, β -strands in orange and loops in green. The C-terminal end of the β -strands is designated by arrowheads. The side chains of the following residues in close contact with the *myo*-inositol ring (labeled Ins) are shown and labeled: His32, Arg69, His82, Lys115, Arg163, Trp178, Asp198, Tyr200 and Asp274. The plot was prepared using the program SETOR (Evans, 1993).

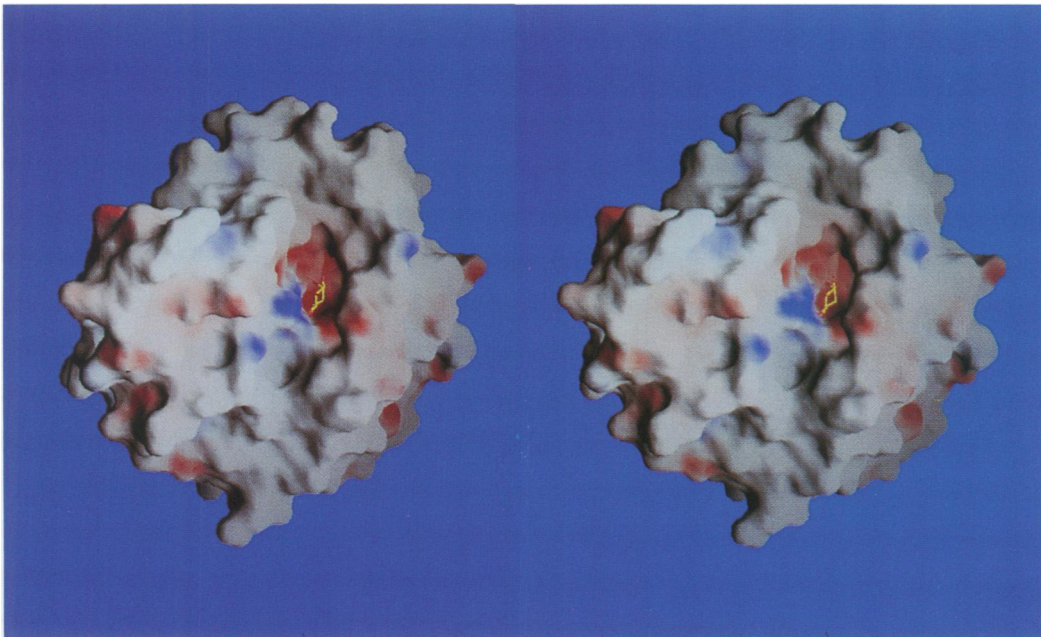


Fig. 6. Stereo picture of an electrostatic surface representation of PI-PLC showing the C-terminal side of the β -barrel with the active site pocket in the center, where negative potentials on the surface are shaded in red and positive potentials in blue. *Myo*-inositol bound to the active site pocket is depicted by yellow bonds. The picture was generated using the program GRASP (Nicholls, 1993).

proteins use similar catalytic tools to cleave identical bonds in otherwise completely different substrates. Structural and kinetic details of mutants at positions 32 and 82 will be described elsewhere. In addition to the two catalytic histidines, the positively charged Arg69 is located in a position suitable to stabilize the pentacovalent transition state during catalysis. Therefore it is very likely that PI-

PLC employs the same catalytic mechanism as observed for the ribonucleases. A scheme of the proposed catalytic mechanism of PI-PLC from *B.cereus* which is consistent with the biochemical evidence and structure is shown in Figure 8. This mechanism is also consistent with the known stereochemistry of the two reactions. The single displacement forming I(1:2cyc)P proceeds with inversion

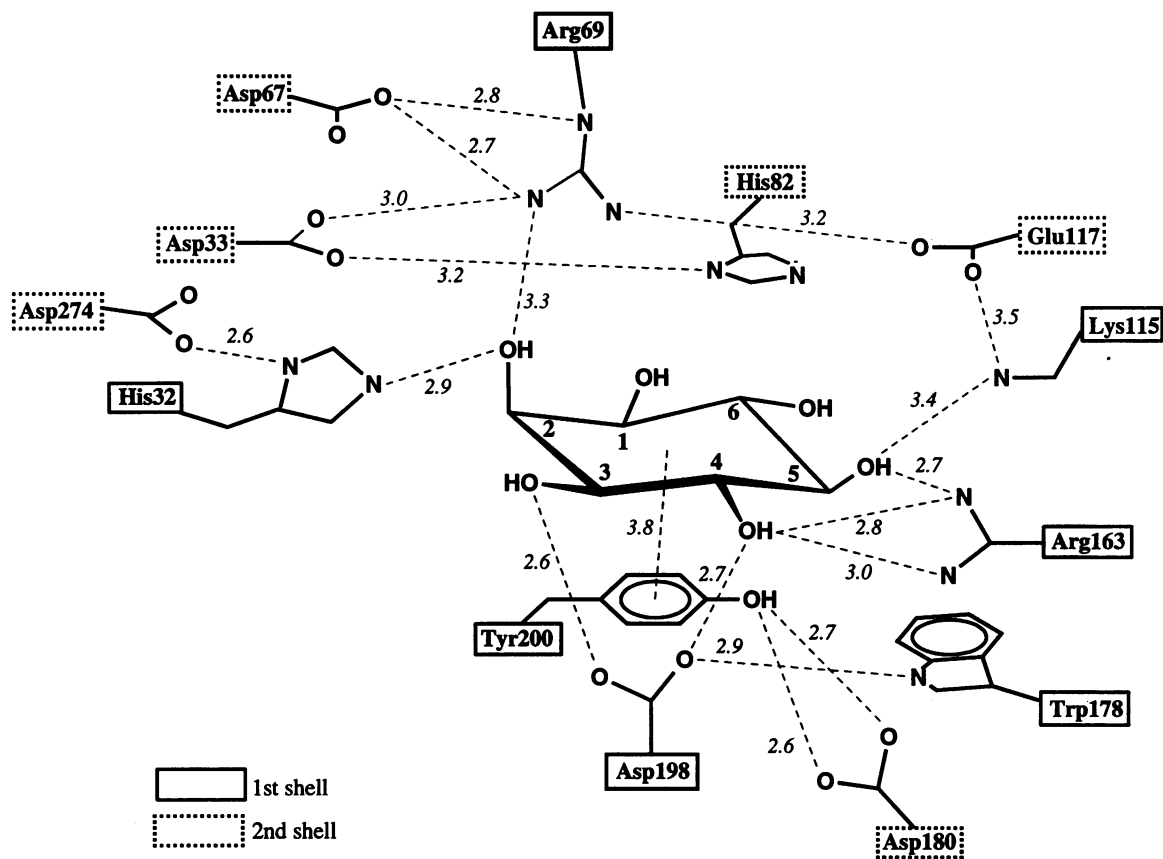


Fig. 7. Schematic drawing of the hydrogen bonding contacts (dashed lines, distances in Å) between the side chains of *B.cereus* PI-PLC residues and *myo*-inositol. Residues belonging to the first and second hydrogen bonding shell are displayed in rectangular and dotted rectangular boxes respectively. The stacking interaction of the phenyl ring of Tyr200 with the *myo*-inositol molecule is also indicated.

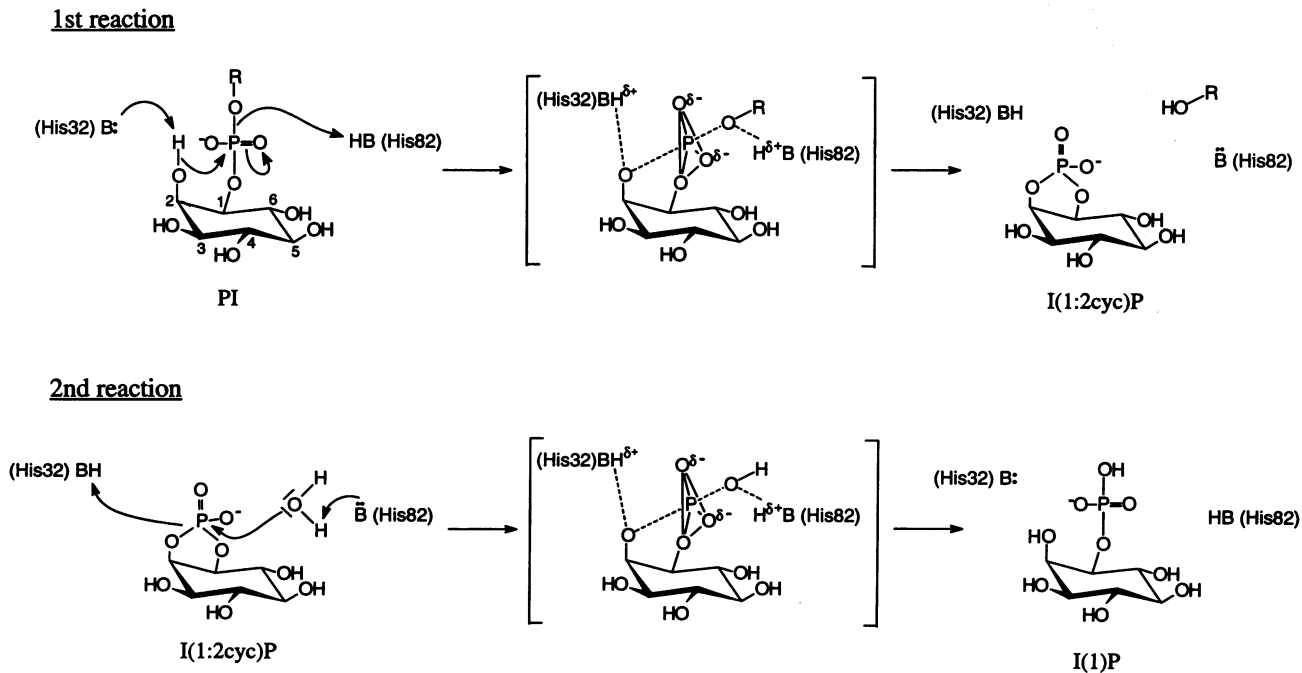


Fig. 8. Proposed catalytic mechanism of the action of *B.cereus* PI-PLC. In the first reaction His32 acts as a general base, accepting a proton from the OH₂ group of the *myo*-inositol moiety of PI, leading to an in-line attack on the phosphorus. At the same time His82 acts as a general acid, donating a proton to the oxygen of the leaving group (R-OH, i.e. DAG). In the second reaction the catalytic roles of His32 and His82 are reversed. Movement of the electrons during the reaction is shown by arrows.

of the configuration at phosphorous and the second reaction forming I(1)P is accompanied by another inversion (Bruzik and Tsai, 1994).

Structure of *B.cereus* PI-PLC as a model for other PI-PLCs?

Common to all PI-PLCs is that they cleave the phosphodiester bond of PI and its glycosylated or phosphorylated derivatives to generate the corresponding I(1:2-cyc)P or a mixture of cyclic and acyclic IPs and DAG. Therefore a similar catalytic mechanism for all PI-PLCs seems plausible (Bruzik and Tsai, 1994). The amino acid sequences for numerous pro- and eukaryotic PI-PLCs are known. The structures of PI-PLC from *B.cereus* and *B.thuringiensis* are essentially identical. The only difference is eight amino acid changes (Kuppe *et al.*, 1989), which are all located on the surface of the enzyme and not directly involved in substrate binding or catalysis. A much lower degree of amino acid conservation is found between the *B.cereus* PI-PLC and the PI-PLCs of *S.aureus* and *L.monocytogenes* (39% and 25% identity, respectively; Leimeister-Wächter *et al.*, 1991; Daugherty and Low, 1993). Nevertheless, the structures of these bacterial enzymes are probably very similar: a high degree of conservation exists for amino acids constituting the hydrophobic core, i.e. the central β -barrel, of the protein. Also, all residues in close contact with the inositol, except for Arg163 in *L.monocytogenes*, are conserved, suggesting a very similar active site and catalytic mechanism for these enzymes. Therefore, the present structure of *B.cereus* PI-PLC can be regarded as the prototype structure for bacterial PI-PLCs with known sequence. This is of considerable interest, because the PI-PLCs from *S.aureus* and *L.monocytogenes* act as potential virulence factors (Leimeister-Wächter *et al.*, 1991; Mengaud *et al.*, 1991; Daugherty and Low, 1993).

The amino acid conservation among the much larger eukaryotic PI-PLCs is very low, with the exception of two regions X and Y of ~170 and 240 amino acids respectively, which show identities of 50–60% for X and ~40% for Y and contain amino acids essential for catalytic activity (Rhee *et al.*, 1989; Bruzik and Tsai, 1994). For residues in the N-terminal half of *B.cereus* PI-PLC (positions 42–123) a relatively high sequence homology (i.e. 26% conservative replacements) with part of region X has been reported (Kuppe *et al.*, 1989). In this alignment His82 is conserved. In another sequence comparison of *B.cereus* PI-PLC (positions 26–161) and region X of several eukaryotic PI-PLCs conservative replacements of ~20% are found, with both His32 and His82 conserved (Mengaud *et al.*, 1991). The importance of two histidines located in region X of mammalian phospholipase C- δ_1 has recently been investigated by mutagenesis (Cheng *et al.*, 1995; Ellis *et al.*, 1995). This includes His356, which is equivalent to His82 in *B.cereus* PI-PLC in several sequence alignments, and His311, which can be aligned with His32. This could be a first indication of a similar catalytic mechanism of prokaryotic and eukaryotic PI-PLCs: a general acid and base catalysis utilizing two conserved histidines.

One important difference between bacterial and mammalian PI-PLCs is that the mammalian PI-PLCs are calcium ion-dependent, whereas the bacterial isozymes, including *B.cereus* PI-PLC, are not. The Ca^{2+} ions in the

mammalian enzymes may be required for the binding of the highly negatively charged PIP_2 , they may play a role in a regulatory domain not present in the much smaller bacterial enzymes or they might stabilize the transition state of the reaction, as observed in small secreted phospholipases A_2 (Scott *et al.*, 1990).

The GPI-PLC of *T.brucei* is similar in size to the bacterial enzymes and does not require calcium for activity. It also shows a relatively high number of conservative substitutions (34%) when compared with the N-terminal half of *B.cereus* PI-PLC and both His32 and His82 appear to be conserved (Carrington *et al.*, 1991).

In summary, we report here the first structure of a PI-PLC. The active site was then identified by determining the structure of the enzyme complexed with a substrate-like inhibitor, *myo*-inositol. The structure provides considerable insight into the catalytic mechanism. In spite of uncertainties in sequence comparisons, the structure of *B.cereus* PI-PLC may well serve as a model not only for other prokaryotic, but also for eukaryotic, PI-PLCs, to increase our understanding of these enzymes and in the design of PI-PLC inhibitors with potential therapeutic use.

Materials and methods

Cloned and overexpressed PI-PLC from *B.cereus* was purified from *Escherichia coli* (Koke *et al.*, 1991) and crystallized in space group $\text{P}2_12_12_1$ with cell dimensions $a = 45.2 \text{ \AA}$, $b = 45.6 \text{ \AA}$ and $c = 160.8 \text{ \AA}$ and $\alpha = \beta = \gamma = 90^\circ$ as described previously (Bullock *et al.*, 1993). Native and derivative data sets were collected from single crystals on a Xoung-Hamlin area detector (Hamlin, 1985) using graphite monochromated $\text{CuK}\alpha$ radiation from a Rigaku RU-200BH rotating anode X-ray generator. Data were processed using the supplied detector software (Howard *et al.*, 1985). Data for the complex between PI-PLC and *myo*-inositol were collected on a Siemens X1000 area detector and processed using the program XDS (Kabsch, 1988). Initially >20 different heavy atom compounds were screened, yielding only three weak derivatives [with heavy atom compounds diacetoxy mercuridipropylene dioxide (DMD), platinum chloride (PtCl_2) and chloro(2,2':6,2''-terpyridinium)-platinum(II) chloride (TERPY); Table I].

To obtain single site mercury derivatives, cysteine residues were introduced into PI-PLC, which is cysteine-free in its native form, by site-directed mutagenesis (Kunkel *et al.*, 1987). Polar residues that showed a high sequence variability among bacterial PI-PLCs, suggesting an exposure of these residues to solvent (Hatfull *et al.*, 1989), were chosen as the target for mutagenesis. Crystals isomorphous to wild-type PI-PLC were grown for four cysteine-containing mutants [Asp139→Cys (D139C), K162C, T185C and D224C] and subsequently soaked in freshly prepared precipitant solution containing 0.1–1 mM HgCl_2 for 3–7 days at 4°C. Mutant K162C gave a single site derivative which allowed the determination of heavy atom sites in the previously uninterpretable derivatives (with heavy atom compounds DMD, PtCl_2 and TERPY) by using difference Fourier methods. The use of these four derivatives resulted in an interpretable electron density map with clear boundaries between the molecule, the solvent and some resolved secondary structure elements. The other cysteine mutant derivatives had three of the four mercury binding sites in common with the DMD derivative. Inclusion of these additional derivatives resulted in further improvement of the electron density map (Table I).

Heavy atom refinement and phase calculation were performed using the program MLPHARE (Otwinowski, 1991) using data to 3.5 Å resolution. Both isomorphous and anomalous difference data were incorporated. Approximately 75% of the polypeptide chain, comprising seven fragments of 10–90 residues in length, was built into the electron density map as a polyalanine backbone using the program O (Jones *et al.*, 1991) and an Evans & Sutherland ESV graphics workstation. These fragments included essentially all secondary structure elements, whereas most of the electron density for loops connecting secondary structure elements remained invisible or uninterpretable. At this point electron density modifications were performed by simultaneous use of the programs SQUASH (Zhang, 1993) and PRISM (Byströff *et al.*,

1993), leading to a map which was of sufficient quality to be able to replace the polyalanine sequence for ~50% of the amino acid residues with the correct sequence.

The model was refined by simulated annealing and conjugate gradient minimization using the program X-PLOR 3.1 (Brünger *et al.*, 1989), employing stereochemical parameters developed by Engh and Huber (1991). The initial partial model (R factor = 44%) was refined by several rounds of positional and simulated annealing refinement and manual rebuilding. The remainder of the sequence was successively built into the electron density map, followed by positional and restrained B factor refinement using data with $I/\sigma_I \geq 1$ from 8.0 to 2.6 Å.

The structure of PI-PLC in complex with its inhibitor *myo*-inositol was determined by difference Fourier techniques and crystallographic refinement using data collected from a single crystal of PI-PLC co-crystallized with 100 mM *myo*-inositol at 4°C and the refined PI-PLC structure as a model for phase calculations (Table I). Prior to inclusion of the inositol molecule in the phase calculations the uncomplexed PI-PLC was refined against the data collected for the complex. The following difference Fourier calculation with coefficient $F_{\text{mut}} - F_{\text{wt}}$ produced a map in which a positive difference density for the inositol molecule was clearly visible. Subsequently *myo*-inositol was built into the map, which was almost unambiguous with respect to the orientation of the inositol ring (Figure 3). Nevertheless, two alternative possible orientations of inositol with respect to the enzyme were also refined, resulting in a poorer stereochemistry and significantly higher temperature factors for the inositol molecule, as well as fewer and less favorable interactions with the enzyme.

Acknowledgements

We thank G.E.Schulz, S.J.Remington and B.W.Matthews for generously providing experimental equipment and for critical comments on the manuscript and C.Vonrhein, U.Baumann, I.Vetter and J.Volwerk for useful discussions. This work was supported in part by NIH grant GM25698 to O.H.G. and a grant from Land Baden-Württemberg to D.W.H.

References

- Aguilar,C.F., Thomas,P.J., Moss,D.S., Mills,A. and Palmer,R.A. (1991) Novel non-productively bound ribonuclease inhibitors—high resolution X-ray refinement studies on the binding of RNase A to cytidyl-2',5'-guanosine (2',5'-CpG) and deoxycytidyl-3',5'-guanosine (3',5'-dCpG). *Biochim. Biophys. Acta*, **1118**, 6–20.
- Bernstein,F.C., Koetzle,T., Williams,G., Meyer,E., Jr, Brice,M., Rodgers,J., Kennard,O., Shimanouchi,T. and Tasumi,M. (1977) The Protein Data Bank: a computer-based archival-file for macromolecular structures. *J. Mol. Biol.*, **112**, 535–542.
- Berridge,M.J. and Irvine,R.F. (1989) Inositol phosphates and cell signalling. *Nature*, **341**, 197–205.
- Brünger,A.T. (1992) Free R value: a novel statistical quantity for assessing the accuracy of crystal structures. *Nature*, **355**, 472–475.
- Brünger,A.T., Karplus,M. and Petsko,G.A. (1989) Crystallographic refinement by simulated annealing: application to crambin. *Acta Crystallogr.*, **A45**, 50–61.
- Bruzik,K.S. and Tsai,M.-D. (1994) Toward the mechanism of phosphoinositide-specific phospholipases C. *Bioorg. Med. Chem.*, **2**, 49–72.
- Bruzik,K.S., Morocho,A.M., Jhon,D.-Y., Rhee,S.G. and Tsai,M.-D. (1992) Phospholipids chiral at phosphorus: stereochemical mechanism for the formation of inositol 1-phosphate catalyzed by phosphatidylinositol-specific phospholipase C. *Biochemistry*, **31**, 5183–5193.
- Bullock,T.L., Ryan,M., Kim,S.L., Remington,S.J. and Griffith,O.H. (1993) Crystallization of phosphatidylinositol-specific phospholipase C from *Bacillus cereus*. *Biophys. J.*, **64**, 784–791.
- Bystroff,C., Baker,D., Fletterick,R.J. and Agard,D.A. (1993) PRISM: application to the solution of two protein structures. *Acta Crystallogr.*, **D49**, 440–448.
- Carrington,M., Walters,D. and Webb,H. (1991) The biology of the glycosyl-phosphatidylinositol-specific phospholipase C of *Trypanosoma brucei*. *Cell Biol. Int. Rep.*, **15**, 1101–1114.
- Cheng,H.-F., Jiang,M.-J., Chen,C.-L., Liu,C.-L., Wong,L.-P., Lomasney,J.W. and King,K. (1995) Cloning and identification of amino acid residues of human phospholipase C δ 1 essential for catalysis. *J. Biol. Chem.*, **270**, 5495–5505.
- Daugherty,S. and Low,M.G. (1993) Cloning, expression, and mutagenesis of phosphatidylinositol-specific phospholipase C from *Staphylococcus aureus*: a potential staphylococcal virulence factor. *Infect. Immun.*, **61**, 5078–5089.
- Ellis,M.V., Sally,U. and Katan,M. (1995) Mutations within a highly conserved sequence present in the X region of phosphoinositide-specific phospholipase C- δ 1. *Biochem. J.*, **307**, 69–75.
- Engh,R.A. and Huber,R. (1991) Accurate bond and angle parameters for X-ray protein structure refinement. *Acta Crystallogr.*, **A47**, 392–400.
- Evans,S.V. (1993) SETOR: hardware lighted three-dimensional solid model representations of macromolecules. *J. Mol. Graphics*, **11**, 134–138.
- Farber,G.K. (1993) An α/β -barrel full of evolutionary trouble. *Curr. Opin. Struct. Biol.*, **3**, 409–412.
- Hamlin,R. (1985) Multiwire area X-ray diffractometers. *Methods Enzymol.*, **114**, 416–452.
- Hatfull,G.F., Sanderson,M.R., Freemont,P.S., Raccuia,P.R., Grindley,N.D.F. and Steitz,T.A. (1989) Preparation of heavy-atom derivatives using site-directed mutagenesis. *J. Mol. Biol.*, **208**, 661–667.
- Hendrickson,H.S., Hendrickson,E.K., Johnson,J.L., Khan,T.H. and Chial,H.J. (1992) Kinetics of phosphatidylinositol-specific phospholipase C with thiophosphate and fluorescent analogues of phosphatidylinositol. *Biochemistry*, **31**, 12169–12172.
- Herold,D., Hart,G.W. and Englund,P.T. (1988) cDNA encoding the glycosyl-phosphatidylinositol-specific phospholipase C of *Trypanosoma brucei*. *Proc. Natl Acad. Sci. USA*, **85**, 8914–8918.
- Hough,E., Hansen,L.K., Birknes,B., Jynge,K., Hansen,S., Hordvik,A., Little,C., Dodson,E. and Derewanda,Z. (1989) High-resolution (1.5 Å) crystal structure of phospholipase C from *Bacillus cereus*. *Nature*, **338**, 357–360.
- Howard,A.J., Nielsen,C. and Xuong,N.H. (1985) Software for a diffractometer with multiwire area detector. *Methods Enzymol.*, **114**, 452–472.
- Ikezawa,H. (1991) Bacterial PIPLCs—unique properties and usefulness in studies on GPI anchors. *Cell Biol. Int. Rep.*, **15**, 1115–1131.
- Jones,T.A., Zhou,J.-Y., Cowan,S. and Kjeldgaard,M. (1991) Improved methods for building protein models in electron density maps and the location of errors in these models. *Acta Crystallogr.*, **A47**, 110–119.
- Kabsch,W. (1988) Evaluation of single-crystal X-ray diffraction data from a position-sensitive detector. *J. Appl. Crystallogr.*, **21**, 916–924.
- Koke,J.A., Yang,M., Henner,D.J., Volwerk,J.J. and Griffith,O.H. (1991) High-level expression in *Escherichia coli* and rapid purification of phosphatidylinositol-specific phospholipase C from *Bacillus cereus* and *Bacillus thuringiensis*. *Protein Expression Purificat.*, **2**, 51–58.
- Kunkel,T.A., Roberts,J.D. and Zakour,R.A. (1987) Rapid and efficient site-specific mutagenesis without phenotypic selection. *Methods Enzymol.*, **154**, 367–382.
- Kuppe,A., Evans,L.M., McMillen,D.A. and Griffith,O.H. (1989) Phosphatidylinositol-specific phospholipase C of *Bacillus cereus*: cloning, sequencing, and relationship to other phospholipases. *J. Bacteriol.*, **171**, 6077–6083.
- Leimeister-Wächter,M., Domann,E. and Chakraborty,T. (1991) Detection of a gene encoding phosphatidylinositol-specific phospholipase C that is co-ordinately expressed with listeriolysin in *Listeria monocytogenes*. *Mol. Microbiol.*, **5**, 361–366.
- Lesk,A.M., Brändén,C.-I. and Chothia,C. (1989) Structural principles of α/β barrel proteins: the packing of the interior of the sheet. *Proteins: Struct. Funct. Genet.*, **5**, 139–148.
- Lewis,K.A., Garigapati,V.R., Zhou,C. and Roberts,M.F. (1993) Substrate requirements of bacterial phosphatidylinositol-specific phospholipase C. *Biochemistry*, **32**, 8836–8841.
- Lin,G., Bennett,F. and Tsai,M.-D. (1990) Phospholipids chiral at phosphorus: stereochemical mechanism of reactions catalyzed by phosphatidylinositol-specific phospholipase C from *Bacillus cereus* and guinea pig uterus. *Biochemistry*, **29**, 2747–2757.
- Lüthy,R., Bowie,J.U. and Eisenberg,D. (1992) Assessment of protein models with three-dimensional profiles. *Nature*, **356**, 83–85.
- Mengaud,J., Braun-Breton,C. and Cossart,P. (1991) Identification of phosphatidylinositol-specific phospholipase C activity in *Listeria monocytogenes*: a novel type of virulence factor? *Mol. Microbiol.*, **5**, 367–372.
- Morris,A.L., MacArthur,M.W. and Thornton,J.N. (1992) Stereochemical quality of protein structure coordinates. *Proteins: Struct. Funct. Genet.*, **12**, 345–364.
- Nicholls,A.J. (1993) *GRASP Manual*. Columbia University, New York, NY.
- Otwinowski,Z. (1991) Maximum likelihood refinement of heavy atom parameters. In Wolf,W., Evans,P.R. and Leslie,A.G.W. (eds),

- Isomorphous Replacement and Anomalous Scattering*. SERC, Daresbury Laboratory, Warrington, UK, pp. 80–86.
- Quioco, F.A. (1989) Protein–carbohydrate interactions: basic molecular features. *Pure Appl. Chem.*, **61**, 1293–1306.
- Renetseder, R., Brunie, S., Dijkstra, B.W., Drenth, J. and Sigler, P.B. (1985) A comparison of the crystal structures of phospholipase A₂ from bovine pancreas and *Crotalus atrox* venom. *J. Biol. Chem.*, **260**, 11627–11634.
- Rhee, S.G., Suh, P.-G., Ryu, S.H. and Lee, S.Y. (1989) Studies of inositol phospholipid-specific phospholipase C. *Science*, **244**, 546–550.
- Richards, F.M. and Wyckoff, H.W. (1971) Bovine pancreatic ribonuclease. In Boyer, P.D. (ed.), *The Enzymes*. Academic Press, New York, NY, pp. 647–806.
- Rouvinen, J., Bergfors, T., Teeri, T., Knowles, J.K.C. and Jones, T.A. (1990) Three-dimensional structure of cellobiohydrolase II from *Trichoderma reesei*. *Science*, **249**, 380–385.
- Scott, D.L., White, S.P., Otwinowski, Z., Yuan, W., Gelb, M.H. and Sigler, P.B. (1990) Interfacial catalysis: the mechanism of phospholipase A₂. *Science*, **250**, 1541–1546.
- Shashidhar, M.S., Volwerk, J.J., Keena, J.F.W. and Griffith, O.H. (1990) Inhibition of phosphatidylinositol-specific phospholipase C by phosphonate substrate analogues. *Biochim. Biophys. Acta*, **1042**, 410–412.
- Sippl, M.J. (1993) Recognition of errors in three-dimensional structures of proteins. *Proteins: Struct. Funct. Genet.*, **17**, 355–362.
- Spezio, M., Wilson, D.B. and Karplus, P.A. (1993) Crystal structure of the catalytic domain of a thermophilic endocellulase. *Biochemistry*, **32**, 9906–9916.
- Suh, P.-G., Ryu, S.H., Moon, K.H., Suh, H.W. and Rhee, S.G. (1988) Cloning and sequence of multiple forms of phospholipase C. *Cell*, **54**, 161–169.
- Thompson, J.E. and Raines, R.T. (1994) Value of general acid–base catalysis to ribonuclease A. *J. Am. Chem. Soc.*, **116**, 5467–5468.
- Turner, A.J. (ed.) (1990) *Molecular and Cell Biology of Membrane Proteins. Glycolipid Anchors of Cell-Surface Proteins*. Ellis Horwood, Chichester, UK, pp. 5–220.
- Volwerk, J.J., Shashidhar, M.S., Kuppe, A. and Griffith, O.H. (1990) Phosphatidylinositol-specific phospholipase C from *Bacillus cereus* combines intrinsic phosphotransferase and cyclic phosphodiesterase activities: a ³¹P NMR study. *Biochemistry*, **29**, 8056–8062.
- Volwerk, J.J., Filthuth, E., Griffith, O.H. and Jain, M.K. (1994) Phosphatidylinositol-specific phospholipase C from *Bacillus cereus*: interfacial binding, catalysis, and activation. *Biochemistry*, **33**, 3464–3474.
- White, S.P., Scott, D.L., Otwinowski, Z., Gelb, M.H. and Sigler, P.B. (1990) Crystal structure of cobra-venom phospholipase A₂ in a complex with a transition-state analogue. *Science*, **250**, 1560–1563.
- Zhang, K.Y.J. (1993) SQUASH—combining constraints for macromolecular phase refinement and extension. *Acta Crystallogr.*, **D49**, 213–222.

Received on April 5, 1995; revised on May 22, 1995